Proinflammatory Activation of Macrophages by Basic Calcium Phosphate Crystals via Protein Kinase C and MAP Kinase Pathways

A Vicious Cycle of Inflammation and Arterial Calcification?

Imad Nadra, Justin C. Mason, Pandelis Philippidis, Oliver Florey, Cheryl D.W. Smythe, Geraldine M. McCarthy, Robert C. Landis, Dorian O. Haskard

Abstract—Basic calcium phosphate (BCP) crystal deposition underlies the development of arterial calcification. Inflammatory macrophages colocalize with BCP deposits in developing atherosclerotic lesions and in vitro can promote calcification through the release of TNF alpha. Here we have investigated whether BCP crystals can elicit a proinflammatory response from monocyte-macrophages. BCP microcrystals were internalized into vacuoles of human monocyte-derived macrophages in vitro. This was associated with secretion of proinflammatory cytokines (TNFα, IL-1β and IL-8) capable of activating cultured endothelial cells and promoting capture of flowing leukocytes under shear flow. Critical roles for PKC, ERK1/2, JNK, but not p38 intracellular signaling pathways were identified in the secretion of TNF alpha, with activation of ERK1/2 but not JNK being dependent on upstream activation of PKC. Using confocal microscopy and adenoviral transfection approaches, we determined a specific role for the PKC-alpha isozyme. The response of macrophages to BCP crystals suggests that pathological calcification is not merely a passive consequence of chronic inflammatory disease but may lead to a positive feed-back loop of calcification and inflammation driving disease progression. **(*Circ Res*. 2005;96:1248-1256.)**

Key Words: atherosclerosis pathophysiology ■ cell biology ■ calcification ■ inflammation ■ macrophage

Coronary artery calcification occurs as part of the atherosclerotic process, and is due to the deposition in the arterial intima of basic calcium phosphate (BCP) crystals, consisting mainly of calcium hydroyapatite ($Ca_{10}(PO_4)_6(OH)_2$) and similar to those that mineralize bone.[1–6] Using electron beam computed tomography, the amount of vessel calcification has been shown to closely correlate with the extent of plaque burden and may predict future coronary events.[7–10] However, although arterial calcification is now accepted to be an active and highly regulated process similar to that of bone ossification,[11–14] it has tended to be seen merely as a surrogate marker for the burden of atherosclerotic disease rather than a contributor to disease progression.

Growing evidence from the study of degenerative arthritis, in which BCP crystals can be found in the majority of affected joints and closely correlate with the extent of joint destruction, suggests a pathogenic role in driving disease.[15,16] Thus, BCP crystals have been shown to activate synovial fibroblasts, inducing cellular proliferation and matrix metalloproteinase (MMP) secretion through a variety of intracellular signaling pathways, including protein kinase C (PKC), ERK1/2 MAP kinase, NFκB, and AP-1.[17–19] Limited studies using murine cells have also demonstrated the ability of macrophages to interact with BCP crystals in vitro, resulting in DNA synthesis and cytokine production.[20,21]

Cells of the monocyte/macrophage lineage form an important part of the innate immune system and play a key role in atherogenesis.[22] Inflammatory mediators derived from monocyte-macrophages, including TNFα, are thought to contribute to the calcification process through the promotion of osteoblastic differentiation and calcification of vascular smooth muscle cells.[23–25] Furthermore, a link between the activated macrophage and the deposition of calcification may help to explain why histological studies have consistently shown plaque macrophages to colocalize with BCP crystal deposits.[26,27] As yet, however, the ability of BCP crystals to directly activate macrophages in the calcified atherosclerotic plaque remains a relatively unexplored possibility. In this

Original received February 17, 2005; revision received April 25, 2005; accepted May 12, 2005.

From the British Heart Foundation Cardiovascular Medicine Unit (I.M., J.C.M., P.P., O.F., C.D.W.S., R.C.L., D.O.H.), Eric Bywaters Centre for Vascular Inflammation, Faculty of Medicine, Imperial College London, Hammersmith Hospital, London; and the Department of Clinical Pharmacology (G.M.M.), The Royal College of Surgeons, Dublin. The current address of R.C.L. is the Edmund Cohen Laboratory for Vascular Research, Chronic Disease Research Centre, Tropical Medicine Research Institute, UWI, Barbados, West Indies.

Correspondence to Dr D.O. Haskard, British Heart Foundation Cardiovascular Medicine Unit, Eric Bywaters Centre for Vascular Inflammation, Faculty of Medicine, Imperial College London, Hammersmith Hospital, Du Cane Rd, London, W12 ONN UK. E-mail d.haskard@imperial.ac.uk

Circulation Research **is available at http://circres.ahajournals.org** **DOI: 10.1161/01.RES.0000171451.88616.c2**

study we have shown for the first time that BCP crystals can interact with and activate human macrophages in a proinflammatory manner via mechanisms involving protein kinase C (PKC)α and ERK1/2 MAP kinase.

Materials and Methods

Antibodies and Other Reagents

Anti-E/P-selectin (1.2B6), VCAM-1 (IE5), and ICAM-1 (6.5B5) antibodies were generated within our group. Anti-PKCα, PKCβI, PKCβII, PKCδ, PKCϵ, and PKCζ antibodies were purchased from Santa Cruz Biotechnology (Santa Cruz, Calif). Anti-PKCγ and anti-PKCθ antibodies were from Transduction Laboratories (Lexington, Ky). Anti-ERK1/2, JNK, and phospho-specific ERK1/2, and JNK antibodies were from Cell Signaling Technology (Beverly, Mass). Secondary antibodies included swine antirabbit-HRP (DAKO, Glostrup, Denmark), sheep antimouse-HRP (Amersham Life Science, Bucks, UK), and goat antirabbit Alexa Fluor-488 (Molecular Probes, Eugene, Ore). GF109203X, SB203580, JNKII, and U0126 inhibitors were purchased from Merk-Biosciences (Nottingham, UK). LY379196 was a gift from Dr. K. Ways (Eli Lilly, Indianapolis, Ind). Myristoylated PKCα/β inhibitor peptide (Myr-Arg-Phe-Ala-Arg-Lys-Gly-Ala-Leu-Arg-Gln-Lys-Asn-Val) was purchased from Promega (Madision, Wis). Human recombinant macrophage colony-stimulating factor (M-CSF) was purchased from Peprotech EC (London, UK). All other reagents were from Sigma-Aldrich (Poole, UK) unless otherwise stated.

BCP Crystal Synthesis and Preparation

BCP crystals were synthesized by a modification of a previously published method involving alkaline hydrolysis of brushite, $CaHPO_4x2H_2O$.[17,28] Mineral prepared by this method contains ≈90% hydroxyapatite and 10% octacalcium phosphate, and has a composite calcium/phosphate molar ratio of 1.3 to 1.45. The mean particle size was <1 μm. Crystals were baked for 2 hours at 200°C before use. Endotoxin levels were quantified by the QCL-1000 Chromogenic LAL test kit (BioWhittaker) and shown to be less than 20 pg/mL ($<$0.2 EU/mL) in a 5.7 mg/mL stock solution. Crystals were suspended in Hanks' buffered salt solution and sonicated for 1 minute before being added to cell cultures using a 10-fold dilution of this stock solution.

Monocyte/Macrophage Isolation and Cell Culture

Human monocytes were isolated from the freshly drawn venous blood of healthy volunteers and differentiated in vitro into macrophages over a period of 7 days as previously described.[29] Cells were stimulated with BCP crystals or vehicle media control for 20 hours at 37°C in humidified atmosphere with 5% CO_2. Supernatants were collected, centrifuged at 350 $\times$ g to remove particulate debris and stored at −70°C before analysis.

Transmission Electron Microscopy and X-Ray Elemental Microanalysis

Transmission electron microscopy and X-Ray elemental microanalysis were performed as detailed in the online data supplement available at http://circres.ahajournals.org.

Enzyme-Linked Immunosorbent Assays

TNFα, IL-1β, IL-8, and MCP-1 levels in macrophage-conditioned media were determined by enzyme-linked immunosorbent assays (R&D Systems). All samples were measured in duplicate, with the results expressed as the mean±SEM cytokine concentration.

Quantitative Real Time Polymerase Chain Reaction (RT-PCR)

Monocytes were differentiated over 7 days into macrophages on a 6 well plate as previously described, followed by stimulation with BCP crystals (300 $\mu g/cm^2$). Cells were then rinsed once with ice-cold PBS to remove any unbound BCP crystals, after which total RNA was extracted. Quantitative reverse-transcription PCR was then performed, as detailed in the online data supplement. Steady-state mRNA levels were expressed as the ratio of mRNA levels of TNFα (relative to GAPDH) in stimulated cells as compared with that of resting cells.

Endothelial Cell Flow Cytometry and Hydrodynamic Shear Flow Adhesion Assay

Human umbilical vein endothelial cells (HUVEC) were obtained from fresh umbilical cords and cultured as previously described.[30] Endothelial cell flow cytometric analysis and hydrodynamic shear flow adhesion assays were performed as detailed in the online data supplement.

Intracellular Signaling Inhibition

Macrophage cell culture medium was replaced with fresh medium containing the specific signaling inhibitor or vehicle control one hour before stimulation. Following 20 hours stimulation, conditioned media or whole-cell lysates were collected and stored at −70°C for later analysis. None of the inhibitors or adenoviruses used at the specified doses had any adverse effects on cell viability as judged by trypan blue exclusion and a MTT cell viability assay (Cell Titer 96 Aqueous One Stop solution, Promega).

Western Blot Analysis

Western blot analysis was performed by SDS-PAGE and semidry transfer onto a PDVF membrane as previously described (see online data supplement).[30]

Confocal Scanning Fluorescent Microscopy

Stimulated cells were fixed with 4% paraformaldehyde for 30 minutes followed by blocking for 30 minutes at 4°C with 1% BSA in HBSS. Cells were permeabilised by sequential treatment with 100% methanol for 10 minutes at 4°C and HBSS containing 0.1% Triton X100 and 5% rabbit serum (DAKO) for 50 minutes at 4°C. Immunostaining was performed using the primary anti-PKCα antibody (10 μg/mL) for 1 hour at room temperature followed by a secondary Alexa-Fluor-488 conjugated antibody (8 μg/mL) for a further 1.5 hours at room temperature in the dark. Fluorescence was analyzed using a Carl Zeiss LSM5-PASCAL laser-scanning microscope (Herts).

Adenovirus Infection of Macrophages

Details of adenovirus amplification, purification, titration, and infection of macrophages are given in the online data supplement.

Statistical Analysis

All data were expressed as the mean of individual experiments±standard error of the mean (SEM). Data were analyzed using a two-tailed paired t test or a one-way analysis of variance (ANOVA) with Dunnett's correction (GraphPad Prism software).

Results

Inflammatory Cytokine Secretion by BCP-Treated Macrophages

Transmission electron microscopy of macrophages treated with BCP crystals for 20 hours showed vacuoles containing structures similar in appearance to previously published images of hydoxyapatite within cells[31,32] (Figure 1). Furthermore, X-ray elemental microanalysis of macrophages that had been cultured with BCP and then washed showed the presence of a new calcium peak, consistent with internalized crystals (online Figure I).

Analysis of the effects of BCP crystal uptake by macrophages from 10 different donors demonstrated concentration-

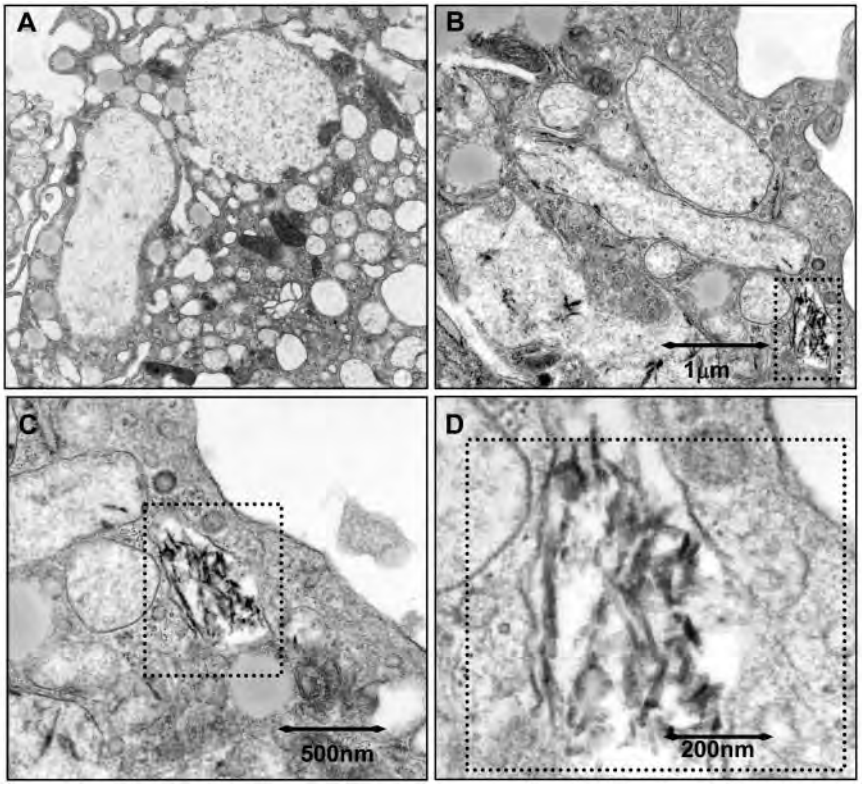

Figure 1. Uptake of BCP crystals by human macrophages. Transmission electron microscopy of (A) an untreated cell demonstrating empty vacuoles and (B, C, and D) cells treated with BCP (300 $\mu g/cm^2$) for 20 hours. The black-dashed box outlines a vacuole containing BCP crystal particles with increasing magnification (A) 8.9 kv, (B) 21kv, (C) 39 kv, and (D) 105 kv.

dependent release of TNFa (312.9±64.9 pg/mL, $P<0.01$) and IL-1β (59.74±29.54 pg/mL, $P<0.05$). TNFα and IL-1β release were dose-dependent with a maximal response at 300 $\mu g/cm^2$. We also found evidence for release of IL-8 (13.75±3.34 ng/mL, $P=0.0034$) but not MCP-1, when tested at a single concentration of BCP crystals (300 mg/mL^2) (Figure 2). A time course revealed slow kinetics of TNFα release with detectable levels first seen after 6 hours, with a continual rise over 48 hours (Figure 3A). TNFα release was dependent on de novo gene transcription and protein translation, as shown by abrogation in the presence of actinomycin D and cycloheximide (both $P<0.01$) (Figure 3B). RT-PCR confirmed that steady-state mRNA levels were raised as early as 1 hour (299.3±116.3) with a continuous rise over 6 hours

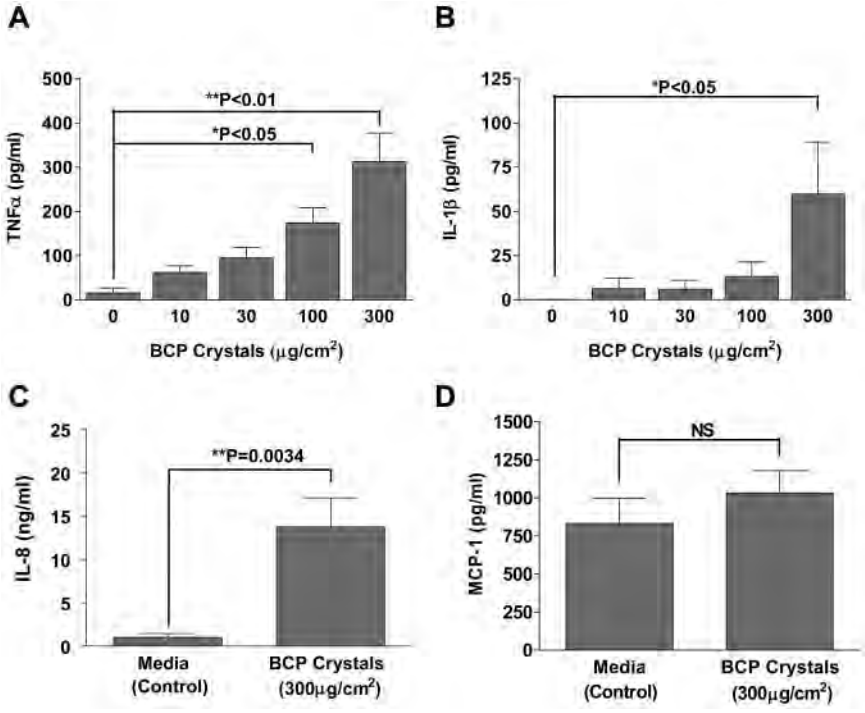

Figure 2. Release of cytokines by human macrophages following stimulation with BCP crystals. Dose response curves for (A) TNFα and (B) IL-1β with increasing doses of BCP (n=10), and significant increase of (C) IL-8, but not (D) MCP-1 in response to stimulation with BCP (300 $\mu g/cm^2$; n=10) for 20 hours.

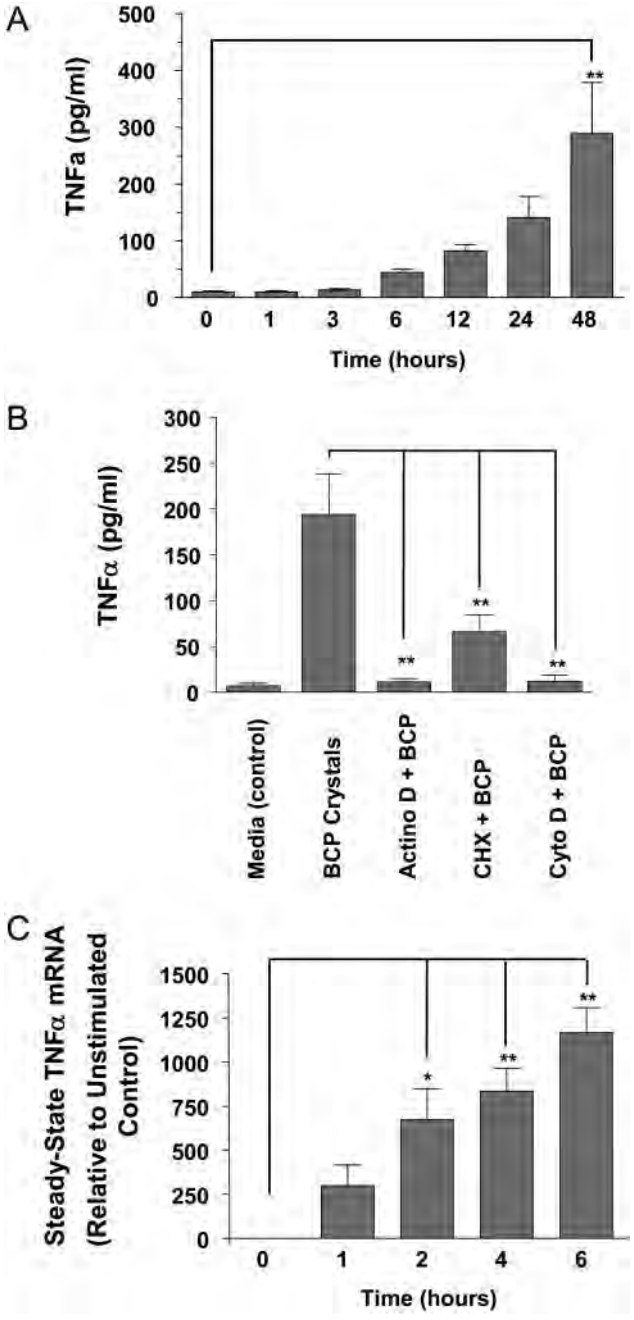

Figure 3. A, Time course of BCP crystal-induced TNFα release by macrophages (n=4); (B) The effect of actinomycin D (ActinoD), cycloheximide (CHX), and cytochalasin D (Cyto D) (each at 1 μg/mL) on TNFα synthesis, (n=5); (C) Quantitative RT-PCR demonstrating the effect of BCP crystals on steady state TNFα mRNA levels (representative experiment of n=3). All experiments were performed using BCP crystals at 300 μg/cm^2. Results are presented as means±SEM (*P<0.05; **P<0.01; One-way ANOVA with Dunnett post test).

(1165±141.4, P<0.01)(Figure 3C). Activation of macrophages by BCP crystals was not secondary to dissolution of BCP crystals raising the calcium and phosphate concentrations, since (i) we found no detectable change in calcium or phosphate concentrations in supernatants of macrophages incubated with BCP crystals for 48 hours; (ii) BCP crystals cultured with macrophages on different sides of a semipermeable membrane did not induce release of TNFα (online Figure II); and (iii) centrifuged supernatants from macrophages cocultured with BCP crystals for 20 hours failed to induce an increase in TNFα mRNA when transferred to fresh macrophage cultures (online Figure III). Unlike TNFα secretion in response to LPS (not shown), the release of TNFα was abrogated by cytochalasin D (P<0.01) (Figure 3B), suggesting the requirement for an intact cytoskeleton.

To establish whether the proinflammatory response of macrophages to BCP was sufficient to activate endothelial cells, HUVEC were coincubated with macrophage-conditioned media and analyzed by flow cytometry for induction of adhesion molecule expression (online Figure IVA). The common epitope on E- and P-selectin recognized by mAb 1.2B6 was upregulated 9-fold after 4 hours and VCAM-1 and ICAM-1 5 and 6-fold respectively after 16 hours. To demonstrate that activated HUVEC were able to support the capture of leukocytes under shear flow, lawns of HUVEC were established in a parallel-plate flow chamber and treated with macrophage-conditioned media for 16 hours before superfusion with mononuclear cells. Conditioned media from BCP treated macrophages promoted a 2.9-fold increase in rolling and a 13.1-fold increase in mononuclear cell arrest at a hydrodynamic shear force of 1.5 dynes/cm^2 (online Figure IVB).

Intracellular Signaling Pathways Stimulated by BCP

Pretreatment with increasing doses of the broad spectrum PKC isozyme inhibitor GF109203X abrogated TNFα production in a dose dependent manner in response to BCP crystals (Figure 4A). At 10 μmol/L of GF109203X, TNFα synthesis was 100% inhibited (272.0±59.4 pg/mL versus 46.7±39.3 pg/mL, P<0.01). Next, the 3 main MAP kinase-signaling pathways, ERK1/2, JNK, and p38, were investigated. Pretreatment with the ERK1/2 inhibitor, U0126, reduced TNFα secretion in a dose-dependent manner, with maximum inhibition of 74% seen at 2.5 μmol/L (487.8±169.2 pg/mL versus 182.3±52.5 pg/mL, P<0.01) (Figure 4B). The role of JNK was demonstrated by dose-dependent inhibition of up to 74% with the JNK inhibitor JNK-II (382.4±86.5 pg/mL versus 128.0±58.9 pg/mL, P<0.01) (Figure 4C). In contrast, inhibition of p38 MAP kinase with concentrations of SB203580 up to 25 μmol/L had no significant inhibitory effect on TNFα production (Figure 4D).

PKCα Activation by BCP

Since the production of TNFα in response to BCP was completely dependent on PKC signaling, we investigated which isozymes(s) of PKC might be involved. In agreement with the previous reports,[33,34] Western blot analysis of unstimulated macrophages indicated the presence of the classical PKCα, β1, β2 but not γ isozymes (Figure 5A). Similarly the atypical PKCζ, the novel PKCδ, and ϵ isozymes, but not θ, were detected. As a positive control, a HUVEC lysate was blotted for the presence of PKC γ and θ, revealing 80 and 79 kDa bands respectively (not shown). As GF109203X inhibits PKCα, β, γ, δ, ϵ isozymes, we further investigated the roles of individual isozymes in the macrophage response to BCP. The involvement of PKCα or PKCβ in BCP-mediated TNFα

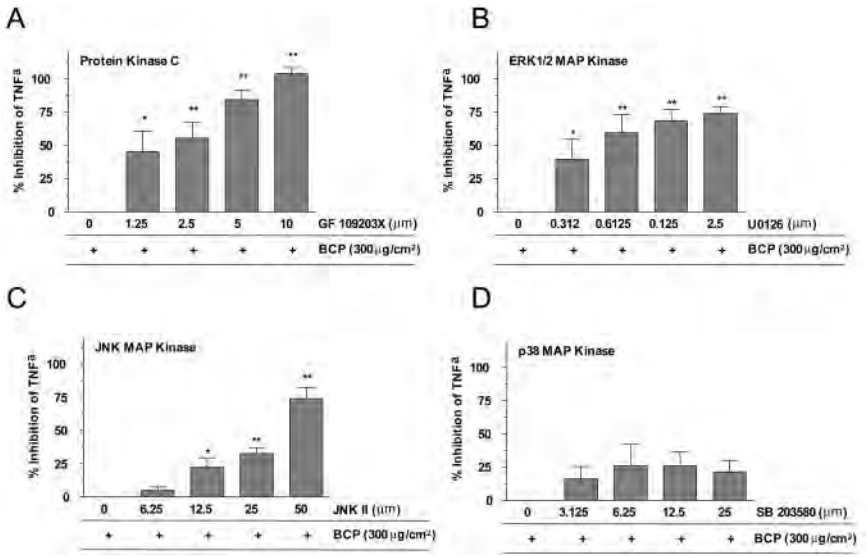

Figure 4. The effect of intracellular signaling pathway inhibitors on BCP induced macrophage TNFα production. The following panel of signaling inhibitors was used: (A) pan-isozyme PKC antagonist, GF109203X (n=5); (B) ERK1/2 pathway MEK1/2 inhibitor U0126 (n=5), (C) JNK MAP Kinase inhibitor JNKII and (D) p38 inhibitor SB203580 (n=6). Results expressed as the percentage inhibition of TNFα production compared with macrophages treated with BCP alone. All experiments were performed using BCP crystals at 300 μg/cm^2. Data are presented as means±SEM, (*P<0.05; **P<0.01; One-way ANOVA with Dunnett post test).

release was first established using a selective and specific myristoylated peptide PKCα/β inhibitor (Figure 5B). Pretreatment with increasing doses of peptide had a partial inhibitory effect of up to 60% with 100 μmol/L of peptide (1225±466.0pg/mL reduced to 503.1±193.0 pg/mL, P<0.01). Similar results were achieved with Gö6976, another PKCα/β isozyme pharmacological antagonist (data not shown). A role for PKCβ was eliminated by the lack of effect with the PKCβ specific inhibitor LY379196 (Figure 5C). Activation of PKCα was investigated by confocal scanning microscopy to examine the subcellular distribution of this isozyme at various time points following treatment with BCP crystals (Figure 5D). This showed that PKCα translocated from the cytoplasm to a membrane-associated distribution within 5 minutes of stimulation. By 20 minutes, PKCα partitioned to numerous discrete vacuoles. Taken together, these data suggest that TNFα secretion involves the PKCα isozyme.

The specific involvement of PKCα was further confirmed by using a PKCα dominant negative (DN) kinase expressed in an adenovirus. Maximal expression of PKCα was seen with a multiplicity of infection (MOI) for the PKCα DN adenovirus of between 200 and 400, as shown by Western blotting (Figure 6A). There was no significant difference in TNFα expression by control GFP-infected versus uninfected cells (Figure 6B). However, infection with the PKCα specific DN adenovirus construct resulted in a significant 72% inhibition of TNFα release (542.5±94.7 pg/mL versus 234.7±42.0 pg/mL, P<0.01). These results demonstrate unequivocally that TNFα release involves the classical PKCα isozyme.

ERK1/2 and JNK MAP Kinase Activation by BCP

The involvement of the ERK1/2 and JNK MAP kinase pathways were further investigated by assessing phosphorylation of these proteins. Phosphorylation of ERK1/2 was shown by Western blotting to take place within 10 minutes of BCP crystal treatment (Figure 7A). Similarly, JNK was

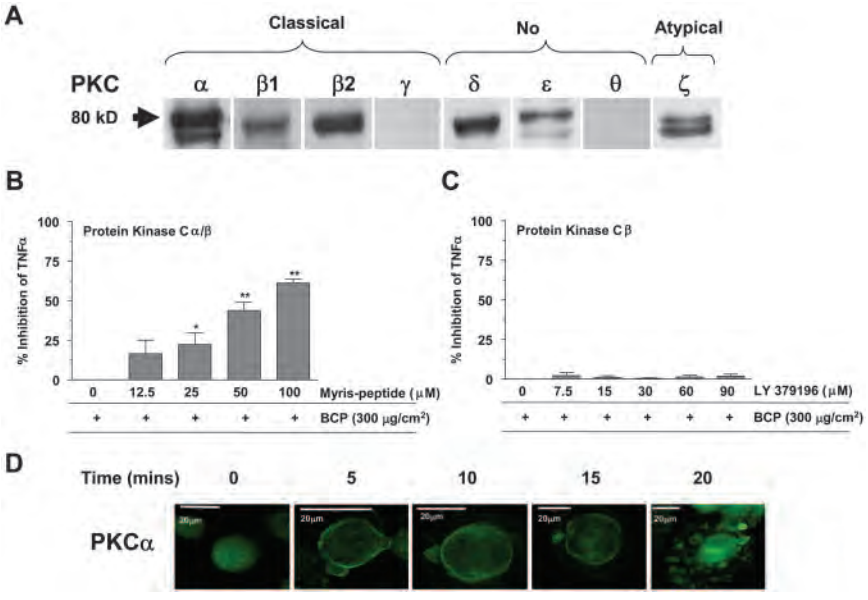

Figure 5. Expression and activation of PKC in human monocyte-derived macrophages. A, Western blot demonstrating the different PKC classical, novel and atypical isozymes present in resting macrophages; B, The effect of PKCα/β isozyme inhibition, using the selective and specific myristoylated PKCα/β inhibitor peptide, on BCP (300 μg/cm^2) induced TNFα production (n=5); C, Effect of PKCβ isozyme inhibition using LY379196 (n=6). Results are expressed as the percentage inhibition of TNFα production compared with macrophages treated with BCP alone. Data are presented as means±SEM, (*P<0.05; **P<0.01; One-way ANOVA with Dunnett post test); D, Translocation of PKCα isozyme on activation of macrophages with calcium BCP crystals (300 μg/cm^2). Subcellular localization of PKCα was imaged by confocal scanning fluorescent microscopy following BCP stimulation. PKCα was initially seen throughout the cytoplasm, and than associated with the extracellular plasma membrane (5 to 15 minutes), followed by movement to vacuoles (20 minutes).

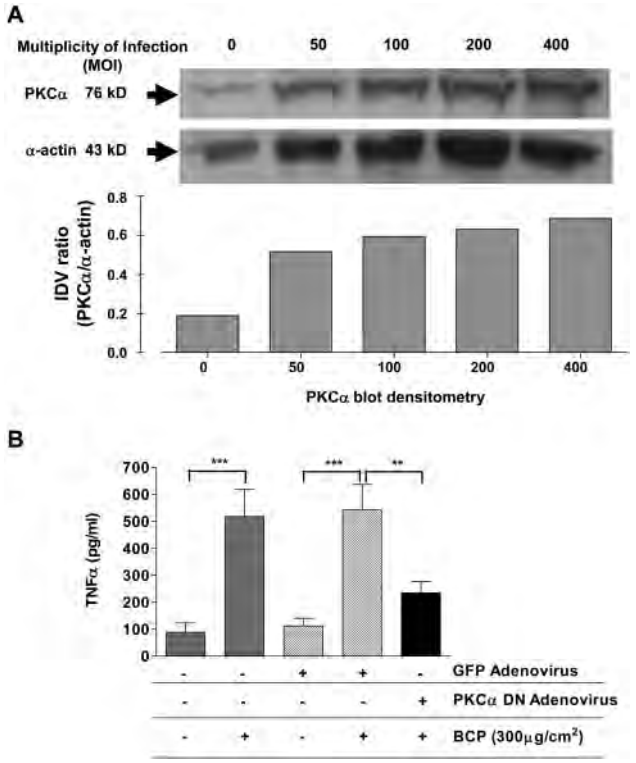

Figure 6. Effect of BCP induced TNFα release in macrophages following infection with PKCα dominant negative kinase expressing adenovirus. A, Western blot demonstrating the expression of PKCα in macrophages following infection with increasing amounts of PKCα dominant negative kinase adenovirus. Representative blot of 2 separate experiments is shown relative to α-actin loading control. The densitometry plot shown below is expressed as the ratio of the integrated density values (IDV) for each band of each blot; B, Effect of adenovirus infection on BCP-induced TNFα release. Macrophages were treated with media (vehicle control) or BCP (300 μg/cm^2). TNFα expression is presented as means±SEM (*P<0.05; **P<0.01; One-way ANOVA with Dunnett post test, n=8 donors).

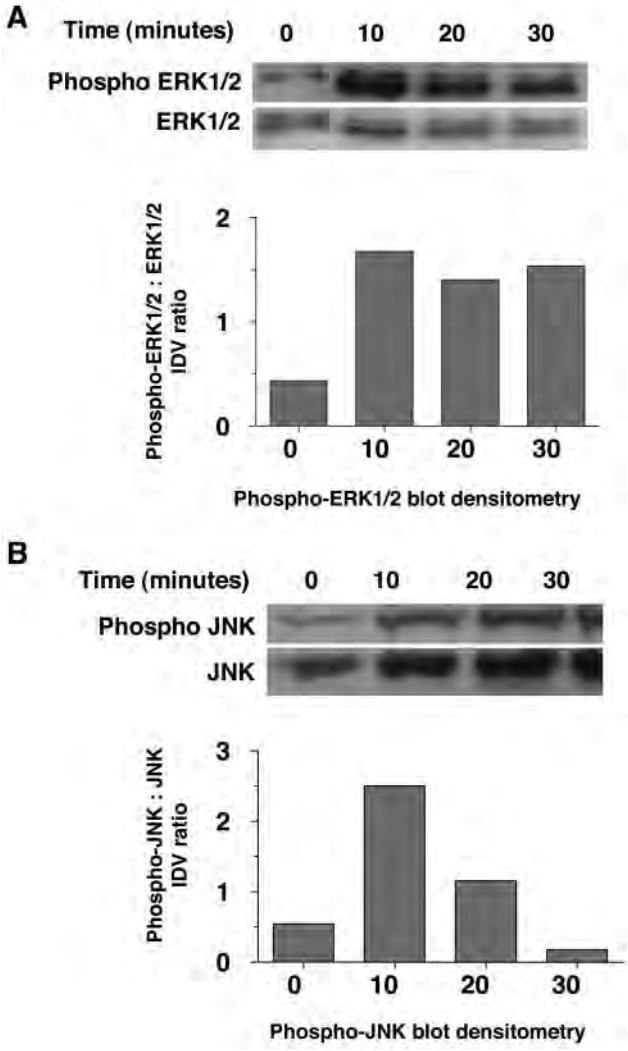

Figure 7. ERK1/2 and JNK MAP kinase signaling pathway activation in response to BCP crystals. Representative blots of 3 separate experiments are shown demonstrating the phosphorylation of (A) ERK1/2 and (B) JNK in human macrophages stimulated with BCP (300 μg/cm^2) for 30 minutes. Blots probed with phosphospecific antibodies were stripped and reprobed with antibodies to native protein to demonstrate equal loading (lower blot).

phosphorylated within 10 minutes, but unlike ERK1/2, was downregulated within 30 minutes (Figure 7B). As the phosphorylation of both these proteins appeared to be maximal at 10 minutes, this time point was investigated in experiments aimed at linking ERK1/2 and JNK signaling with prior PKC activation. Pretreatment with PKC inhibitor GF109203X inhibited ERK1/2 phosphorylation (Figure 8A), whereas no effect on the phosphorylation of JNK was seen (Figure 8B).

Discussion

The presence of arterial calcification has tended to been viewed either as a passive bystander phenomenon or as a useful clinical marker of atherosclerotic disease progression. Here we clearly demonstrate an active inflammatory response by macrophages to BCP crystals with implications for atherosclerosis disease pathogenesis and treatment. We have shown that human macrophages interact with BCP crystals, apparently taking them into vacuoles. In response, macrophages secrete biologically significant quantities of the proinflammatory cytokines TNFα, IL-1β, and IL-8, which are capable of stimulating the activation of endothelial cells and recruitment of mononuclear cells in an in vitro hemodynamic flow assay. Since TNFα can promote osteoblastic differentiation and calcification of vascular cells,[23–25] our data suggest a positive feedback loop predisposing to chronic inflammatory pathology. The model we propose may be of more relevance to intimal than medial calcification, in which the proximity of calcific deposits to macrophages is less clear and in which there may be separate calcification mechanisms.[35]

Scanning electron microscopy of BCP particles extracted from atherosclerotic arteries has revealed marked heterogeneity of shape and size,[2] and it remains to be determined whether these physical characteristics influence macrophage inflammatory responsiveness. In preliminary experiments we have found that the macrophage activating potential of BCP particles is inversely correlated with their size, suggesting that small isolated calcific particles in early disease may be more proinflammatory than larger deposits resembling bone

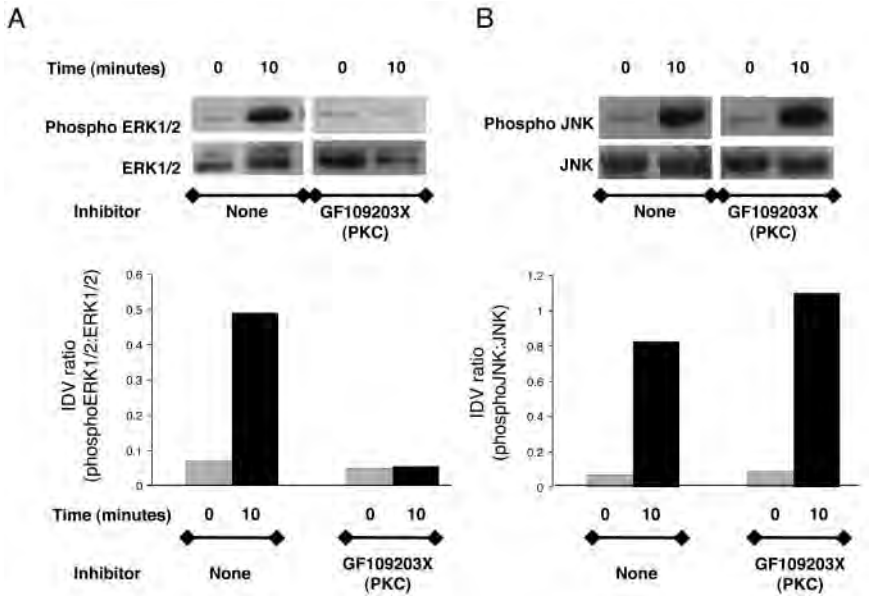

Figure 8. Effect of PKC inhibition on the BCP crystal-induced MAP kinase activation. Phosphorylation of (A) ERK1/2 or (B) JNK over 10 minutes following stimulation with BCP crystals (300 $\mu g/cm^2$) was examined in human macrophages using a phosphospecific antibody. Cells were either treated directly (no inhibitor) or following the pre-incubation with the PKC inhibitor (GF109203X). Representative ERK1/2 or JNK phospho-blot of 3 separate experiments are shown along with membranes stripped and reprobed with antibodies to native ERK1/2 or JNK to demonstrate equal loading (second row).

seen in established lesions.[26,36] If so, it is possible that the inflammatory calcification paradigm we propose is of particular relevance to the progression of early atherosclerosis.

Although the amount of arterial calcification may predict coronary events, it is still unclear whether calcified plaques are more prone to rupture.[7–10] Nevertheless, the biological response to BCP crystals could promote plaque instability. Thus, several studies have demonstrated that BCP is capable of inducing fibroblast MMP production via PKCα and ERK1/2 signaling mechanisms.[19,37] In preliminary experiments we have not been able to show increased expression of MMP-2 or -9 in BCP crystal stimulated macrophages. Nevertheless, BCP crystals might lead to increased tissue proteinase expression and activation by acting on macrophages under conditions so far untested, or indirectly via the effects of macrophage-derived TNFα on vascular smooth muscle cells (VSMC).[38] Furthermore, besides contributing to leukocyte recruitment, macrophage-derived TNFα might also destabilise plaque by contributing to VSMC apoptosis.[39]

It is increasingly recognized that macrophages are not always proinflammatory but may play a role in resolution and repair.[40] Thus we and others have demonstrated a more antiinflammatory profile of cytokine expression in response to other particulate stimuli, such as apoptotic neutrophils, monosodium-urate crystals, and hemoglobin-haptoglobin complexes.[41–43] The differences in the receptor and signaling mechanisms responsible for the variable response of macrophages to these particles requires further study.

A surface receptor responsible for the uptake of BCP crystals by cells has not yet been identified, and it is possible that signal transduction may be mediated by proteins opsonised by crystals rather than by the crystal surface per se. The effects we have observed, however, appear not to be secondary to dissolution of BCP crystals raising the calcium and phosphate concentrations, since we found no detectable change in calcium or phosphate concentrations in supernatants of BCP-macrophage cocultures, and centrifuged supernatants from macrophages cocultured with BCP crystals count not reproduce the effects. Judging from an experiment culturing BCP crystals with macrophages on different sides of a semipermeable membrane, contact between the particles and macrophages is required. However contact is not sufficient, since TNFα release was blocked by inhibiting the cytoskeleton with cytochalasin-D.

We have unequivocally identified PKCα as a key regulator of BCP-induced TNFα release. Several studies have demonstrated an active role for this isoenzyme in the development of phagolysosomes by macrophages in response to microorganisms and other stumili.[44–47] Similarly, our confocal microscopy data demonstrate that BCP crystals stimulate the rapid translocation of PKCα, first to the plasma membrane and then to vacuoles, consistent with PKCa activation being a critical link for downstream signaling. It remains to be determined whether these vacuoles are truly intracellular, or similar to the surface-connected compartments that take up aggregated LDL.[48]

Our data show that both the ERK1/2 and the JNK kinase pathways are involved in BCP-induced TNFα release, but that only ERK1/2 is dependent on upstream PKC activation. These data are consistent with several similar observations in human monocytic cells in response to other agonists.[49–51] Interestingly, there appears to be cell specificity in the macrophage response to BCP, as BCP crystal-induced activation of ERK1/2 in fibroblasts has been found to be dependent on PKCμ rather than a calcium-dependent PKC.[19,52] A recent study in human macrophages described the release of TNFα in response to phorbol ester or LPS, mediated through ERK1/2 via the upstream activation of one of the conventional PKC isozymes, α or β.[53] Importantly, that study demonstrated differential effects on proinflammatory versus antiinflammatory cytokine secretion depending on whether conventional PKC (α or β) or atypical PKCζ isozymes were activated. Based on the conclusions of this study, therapeutic blockade of PKCα isozyme might result in blockade of proinflammatory cytokine production but also a switch to antiinflammatory cytokine production.

In conclusion, through investigation of the mechanisms regulating TNFα production, we have identified key roles for PKCα, ERK1/2, and JNK in downstream signaling in response to BCP crystals. This raises the possibility that specific targeting of such upstream signaling pathways may represent a more effective strategy than blocking TNFα, a downstream product of the inflammatory cascade. Specifically, the identification of PKCα as a proximal signaling molecule makes this a possible therapeutic target for the development of novel treatments against arterial calcification and other calcification-related chronic inflammatory diseases.

Acknowledgments

The study was funded by the British Heart Foundation.

References

1. Carlstrom D, Engfeldt B, Engstrom A, Ringertz N. Studies on the chemical composition of normal and abnormal blood vessel walls. I. Chemical nature of vascular calcified deposits. *Lab Invest*. 1953;2:325–335.
2. Schmid K, McSharry WO, Pameijer CH, Binette JP. Chemical and physicochemical studies on the mineral deposits of the human atherosclerotic aorta. *Atherosclerosis*. 1980;37:199–210.
3. Fitzpatrick LA, Severson A, Edwards WD, Ingram RT. Diffuse calcification in human coronary arteries: association of osteopontin with atherosclerosis. *J Clin Invest*. 1994;94:1597–1604.
4. Guo W, Morrisett JD, DeBakey ME, Lawrie GM, Hamilton JA. Quantification in situ of crystalline cholesterol and calcium phosphate hydroxyapatite in human atherosclerotic plaques by solid-state magic angle spinning NMR. *Arterioscler Thromb Vasc Biol*. 2000;20:1630–1636.
5. Buschman HP, Deinum G, Motz JT, Fitzmaurice M, Kramer JR, van der LA, Bruschke AV, Feld MS. Raman microspectroscopy of human coronary atherosclerosis: biochemical assessment of cellular and extracellular morphologic structures in situ. *Cardiovasc Pathol*. 2001;10:69–82.
6. Jin H, Ham K, Chan JY, Butler LG, Kurtz RL, Thiam S, Robinson JW, Agbaria RA, Warner IM, Tracy RE. High resolution three-dimensional visualization and characterization of coronary atherosclerosis in vitro by synchrotron radiation X-ray microtomography and highly localized x-ray diffraction. *Phys Med Biol*. 2002;47:4345–4356.
7. Wexler L, Brundage B, Crouse J, Detrano R, Fuster V, Maddahi J, Rumberger J, Stanford W, White R, Taubert K. Coronary artery calcification: pathophysiology, epidemiology, imaging methods, and clinical implications. A statement for health professionals from the Am Heart Association. Writing Group. *Circulation*. 1996;94:1175–1192.
8. Arad Y, Spadaro LA, Goodman K, Newstein D, Guerci AD. Prediction of coronary events with electron beam computed tomography. *J Am Coll Cardiol*. 2000;36:1253–1260.
9. Shaw LJ, Raggi P, Schisterman E, Berman DS, Callister TQ. Prognostic value of cardiac risk factors and coronary artery calcium screening for all-cause mortality. *Radiology*. 2003;228:826–833.
10. Thompson GR, Partridge J. Coronary calcification score: the coronary-risk impact factor. *Lancet*. 2004;363:557–559.
11. Tyson KL, Reynolds JL, McNair R, Zhang Q, Weissberg PL, Shanahan CM. Osteo/chondrocytic transcription factors and their target genes exhibit distinct patterns of expression in human arterial calcification. *Arterioscler Thromb Vasc Biol*. 2003;23:489–494.
12. Doherty TM, Asotra K, Fitzpatrick LA, Qiao JH, Wilkin DJ, Detrano RC, Dunstan CR, Shah PK, Rajavashisth TB. Calcification in atherosclerosis: bone biology and chronic inflammation at the arterial crossroads. *Proc Natl Acad Sci U S A*. 2003;100:11201–11206.
13. Abedin M, Tintut Y, Demer LL. Vascular calcification: mechanisms and clinical ramifications. *Arterioscler Thromb Vasc Biol*. 2004;24:1161–1170.
14. Speer MY, Giachelli CM. Regulation of cardiovascular calcification. *Cardiovasc Pathol*. 2004;13:63–70.
15. Schumacher HR Jr. Crystals, inflammation, and osteoarthritis. *Am J Med*. 1987;83:11–16.
16. Molloy ES, McCarthy GM. Hydroxyapatite deposition disease of the joint. *Curr Rheumatol Rep*. 2003;5:215–221.
17. McCarthy GM, Augustine JA, Baldwin AS, Christopherson PA, Cheung HS, Westfall PR, Scheinman RI. Molecular mechanism of basic calcium phosphate crystal-induced activation of human fibroblasts. Role of nuclear factor κB, activator protein 1, and protein kinase C. *J Biol Chem*. 1998;273:35161–35169.
18. Brogley MA, Cruz M, Cheung HS. Basic calcium phosphate crystal induction of collagenase 1 and stromelysin expression is dependent on a p42/44 mitogen-activated protein kinase signal transduction pathway. *J Cell Physiol*. 1999;180:215–224.
19. Reuben PM, Brogley MA, Sun Y, Cheung HS. Molecular mechanism of the induction of metalloproteinases 1 and 3 in human fibroblasts by basic calcium phosphate crystals. Role of calcium-dependent protein kinase C alpha. *J Biol Chem*. 2002;277:15190–15198.
20. Meng ZH, Hudson AP, Schumacher HRJ, Baker JF, Baker DG. Monosodium urate, hydroxyapatite, and calcium pyrophosphate crystals induce tumor necrosis factor-alpha expression in a mononuclear cell line. *J Rheumatol*. 1997;24:2385–2388.
21. Hamilton JA, McCarthy G, Whitty G. Inflammatory microcrystals induce murine macrophage survival and DNA synthesis. *Arthritis Research*. 2001;3:242–246.
22. Greaves DR, Gordon S. Thematic review series: The Immune System and Atherogenesis. Recent insights into the biology of macrophage scavenger receptors. *J Lipid Res*. 2005;46:11–20.
23. Tintut Y, Patel J, Parhami F, Demer LL. Tumor necrosis factor-alpha promotes *in vitro* calcification of vascular cells via the cAMP pathway. *Circulation*. 2000;102:2636–2642.
24. Tintut Y, Patel J, Territo M, Saini T, Parhami F, Demer LL. Monocyte/macrophage regulation of vascular calcification in vitro. *Circulation*. 2002;105:650–655.
25. Shioi A, Katagi M, Okuno Y, Mori K, Jono S, Koyama H, Nishizawa Y. Induction of bone-type alkaline phosphatase in human vascular smooth muscle cells: roles of tumor necrosis factor-alpha and oncostatin M derived from macrophages. *Circ Res*. 2002;91:9–16.
26. Jeziorska M, McCollum C, Woolley DE. Calcification in atherosclerotic plaque of human carotid arteries: associations with mast cells and macrophages. *J Pathol*. 1998;185:10–17.
27. Stary HC. Natural history of calcium deposits in atherosclerosis progression and regression. *Z Kardiol* 2000;89:28–35.
28. Bett JAS, Christner LG, Hall WK. Studies of the hydrogen held by solid XII hydroxyapatite catalysts. *J Am Chem Soc*. 1967;89:5535–5541.
29. Landis RC, Yagnik DR, Florey O, Philippidis P, Emons V, Mason JC, Haskard DO. Safe disposal of inflammatory monosodium urate monohydrate crystals by differentiated macrophages. *Arthritis Rheum*. 2002;46:3026–3033.
30. Mason JC, Yarwood H, Tarnok A, Sugars K, Harrison AA, Robinson PJ, Haskard DO. Human Thy-1 is cytokine-inducible on vascular endothelial cells and is a signaling molecule regulated by protein kinase C. *J Immunol*. 1996;157:874–883.
31. Falasca GF, Ramachandrula A, Kelley KA, O'Connor CR, Reginato AJ. Superoxide anion production and phagocytosis of crystals by cultured endothelial cells. *Arthritis Rheum*. 1993;36:105–116.
32. Hirsch RS, Smith K, Vernon-Roberts B. A morphological study of macrophage and synovial cell interactions with hydroxyapatite crystals. *Ann Rheum Dis*. 1985;44:844–851.
33. Webb BL, Hirst SJ, Giembycz MA. Protein kinase C isoenzymes: a review of their structure, regulation and role in regulating airways smooth muscle tone and mitogenesis. *Br J Pharmacol*. 2000;130:1433–1452.
34. Monick MM, Carter AB, Gudmundsson G, Geist LJ, Hunninghake GW. Changes in PKC isoforms in human alveolar macrophages compared with blood monocytes. *Am J Physiol*. 1998;275:L389–L397.
35. Vattikuti R, Towler DA. Osteogenic regulation of vascular calcification: an early perspective. *Am J Physiol Endocrinol Metab*. 2004;286:E686–E696.
36. Hunt JL, Fairman R, Mitchell ME, Carpenter JP, Golden M, Khalapyan T, Wolfe M, Neschis D, Milner R, Scoll B, Cusack A, Mohler ER III. Bone formation in carotid plaques: a clinicopathological study. *Stroke* 2002;33:1214–1219.
37. McCarthy GM. Calcium crystals and cartilage damage. *Curr Opin Rheumatol*. 1996;8:255–258.
38. Galis ZS, Muszynski M, Sukhova GK, Simon-Morrissey E, Unemori EN, Lark MW, Amento E, Libby P. Cytokine-stimulated human vascular smooth muscle cells synthesize a complement of enzymes required for extracellular matrix digestion. *Circ Res*. 1994;75:181–189.
39. Boyle JJ, Weissberg PL, Bennett MR. Tumor necrosis factor-alpha promotes macrophage-induced vascular smooth muscle cell apoptosis by

direct and autocrine mechanisms. *Arterioscler Thromb Vasc Biol*. 2003; 23:1553–1558.
40. Gordon S. Alternative activation of macrophages. *Nat Rev Immunol*. 2003;3:23–35.
41. Fadok VA, Bratton DL, Konowal A, Freed PW, Westcott JY, Henson PM. Macrophages that have ingested apoptotic cells in vitro inhibit proinflammatory cytokine production through autocrine/paracrine mechanisms involving TGF-beta, PGE2, and PAF. *J Clin Invest*. 1998;101: 890–898.
42. Yagnik DR, Evans BJ, Florey O, Mason JC, Landis RC, Haskard DO. Macrophage release of transforming growth factor (TGF) β1 in the resolution of monosodium urate monohydrate (MSU) crystal-induced inflammation. *Arthritis Rheum*. 2004;50:2273–2280.
43. Philippidis P, Mason JC, Evans BJ, Nadra I, Taylor KM, Haskard DO, Landis RC. Hemoglobin scavenger receptor CD163 mediates interleukin-10 release and heme oxygenase-1 synthesis: anti-inflammatory monocyte-macrophage responses *in vitro*, in resolving skin blisters *in vivo* and Postoperatively following cardio-pulmonary bypass. *Circ Res*. 2004;94:119–126.
44. Allen LH, Aderem A. A role for MARCKS, the alpha isozyme of protein kinase C and myosin I in zymosan phagocytosis by macrophages. *J Exp Med*. 1995;182:829–840.
45. St-Denis A, Caouras V, Gervais F, Descoteaux A. Role of protein kinase C-alpha in the control of infection by intracellular pathogens in macrophages. *J Immunol*. 1999;163:5505–5511.
46. Holm A, Tejle K, Gunnarsson T, Magnusson KE, Descoteaux A, Rasmusson B. Role of protein kinase C alpha for uptake of unopsonized prey and phagosomal maturation in macrophages. *Biochem Biophys Res Commun*. 2003;302:653–658.
47. Ng Yan Hing JD, Desjardins M, Descoteaux A. Proteomic analysis reveals a role for protein kinase C-alpha in phagosome maturation. *Biochem Biophys Res Commun*. 2004;319:810–816.
48. Zhang WY, Gaynor PM, Kruth HS. Aggregated low density lipoprotein induces and enters surface-connected compartments of human monocyte-macrophages. Uptake occurs independently of the low density lipoprotein receptor. *J Biol Chem*. 1997;272:31700–31706.
49. Kontny E, Ziolkowska M, Ryzewska A, Maslinski W. Protein kinase C-dependent pathway is critical for the production of pro-inflammatory cytokines (TNF-alpha, IL-1beta, IL-6). *Cytokine*. 1999;11:839–848.
50. Kurosawa M, Numazawa S, Tani Y, Yoshida T. ERK signaling mediates the induction of inflammatory cytokines by bufalin in human monocytic cells. *Am J Physiol Cell Physiol*. 2000;278:C500–C508.
51. Park H, Park SG, Kim J, Ko YG, Kim S. Signaling pathways for TNF production induced by human aminoacyl-tRNA synthetase-associating factor, p43. *Cytokine*. 2002;20:148–153.
52. Reuben PM, Sun Y, Cheung HS. Basic calcium phosphate crystals activate p44/42 MAPK signal transduction pathway via protein kinase Cmicro in human fibroblasts. *J Biol Chem*. 2004;279:35719–3571925.
53. Foey AD, Brennan FM. Conventional protein kinase C and atypical protein kinase C zeta differentially regulate macrophage production of tumour necrosis factor-alpha and interleukin-10. *Immunology*. 2004;112: 44–53.

ONLINE DATA SUPPLEMENT

ONLINE METHODS

Transmission electron microscopy

Macrophages were washed and detached by incubating with 2.5mM EDTA for 20 mins at 4ºC. The cells were washed and fixed for 2 hours in 3.5 % glutaraldehyde, 0.1M sodium cacodylate buffer. Fixed cells were pelleted and dehydrated by passage through a graded series of ethanol solutions to absolute ethanol followed by exposure to propylene oxide, 50/50 propylene oxide and Spurr resin and a final 4 hours in Spurr resin to impregnate the cells. Samples embedded in Spurr resin were polymerized overnight at 60ºC. 80nm sections were collected on nickel-300 mesh grids and stained with uranyl acetate/lead citrate prior to examination with a Philips-CM10 transmission electron microscope (Philips, Cambridge, UK) at 80 KV

X-ray elemental microanalysis

Cells were cultured on Thermanox™ cover slips (Nalge Nunc International, Roskilde, Denmark) placed in flat bottomed 24 well tissue culture plates. Following stimulation of cells for 18 hours, samples were vigorously washed three times with room temperature PBS to remove excess BCP crystals, before being fixed for 2 hours in 3 % glutaraldehyde in 0.1M sodium cacodylate buffer. Fixative was then removed and cells were stored in 0.1M sodium cacodylate buffer at 4ºC. Fixed samples were dehydrated by passage through a graded series of ethanol solutions to absolute ethanol and critical point dried through liquid CO_2. Cover slips were fixed to aluminium stubs with carbon adhesive tabs and finally sputter coated with gold. X-ray microanalysis of elemental composition was performed within a Stereoscan 360 scanning electron microscope (Lecia Cambridge, Cambridge, UK). The emission X-

ray spectra were measured during the interaction of the primary electron beam with the sample. Elemental composition of the sample was determined by comparison of the emitted X-ray energy spectra of the samples with known energy characteristics of different elements.

Quantitative real time polymerase chain reaction (RT-PCR)

Monocytes were differentiated over seven days into macrophages on a six well plate as described above, followed by stimulation with BCP crystals (300μg/cm^2). Cells were then rinsed once with ice cold PBS to remove any unbound BCP crystals and total RNA was extracted using the Qiagen RNeasy® mini prep kit (Qiagen, West Sussex, UK). Quantitative reverse-transcription PCR was then performed, as detailed in Online Data Supplement. Total RNA extracted was then quantified from the absorbance readings taken at $A_{260\ nm}$ using an Ultrospec 3000, UV/Visible spectrophotometer, (Amersham Biosciences, Bucks, UK). For reverse transcription, 1μg of total RNA was added to a mixture containing 0.5μg oligo (dT)12-18 (MWG-Biotech, Milton Keynes, UK), 1μl of PCR nucleotide mix (10mM each dNTP, Roche, USA) and made up to a final volume of 12μl using DEPC-treated water. Mixture was heated at 65°C for 5 minutes and then snap-cooled on ice for a further 5 minutes. The following reaction components were then added to each tube: 4 μl of 5x first strand PCR buffer, 2μl 0.1M DTT and 1μl of DEPC-treated water to a final volume of 19μl. Reaction tubes were then heated at 42°C for two minutes followed by the addition of 200units of Superscript™ II RNase H$^-$ reverse transcriptase (Invitrogen, Carlsbad, Ca, USA) to make a final reaction volume of 20μl. Reaction mixture was heated for a further 50 minutes at 42°C followed by 70°C for 15 minutes to inactivate the reverse transcriptase enzyme. The cDNA products were stored at -20°C until used for

quantitative PCR analysis. Quantitative RT-PCR was then performed using a Bio-Rad thermal cycler fitted to the iCycler iQ real-time detection system (Bio Rad, Herts, UK). Target sequence primer pairs for the TNFα (Hs00174128_m1) and the house keeping gene GAPDH (Hs99999905_m1) were purchased as pre-designed and pre-optimised Taqman® Assays-on-demand products from Applied Biosystems (Foster City, CA, USA). cDNA template was diluted 1:20 with DEPC-treated water. 1μl of diluted cDNA was then added to 1.25μl Assay-on-demand primer, 12.5μl Master mix (Applied Biosystems, Foster City, CA, USA) and made up to a total reaction volume of 25μl with DEPC-treated water. Reaction mixture was then placed on optical RT-PCR plates in triplicate (Applied Biosystems, Foster City, CA, USA) and run through a PCR amplification sequence of 2 minutes at 50°C, followed by 10 minutes at 95°C and then 40 consecutive denature (15 seconds at 95°C) and anneal/extend (1 minute at 56°C) cycles. Dilution experiments of cDNA template were performed and PCR reaction efficiencies determined using the Bio-Rad iCycler software to ensuring that both primer pairs were comparable (PCR efficiencies were TNFα 89.8% and GAPDH 86.6%). Similarly the optimal temperature for the anneal/extension step of the PCR reaction was determined to be 56°C for both the TNFα and GAPDH gene assay-on-demand primer pairs. Calculation of steady state mRNA levels was performed using the $2^{-\Delta\Delta C_T}$ method, according to the ABI User #2 Bulletin and as previously described [1]. Using this method steady state mRNA levels were expressed as the ratio of mRNA levels of TNFα (relative to GAPDH) in stimulated cells as compared to that of resting cells.

Endothelial cell flow cytometric analysis

Human umbilical vein endothelial cells (HUVEC) were obtained from fresh umbilical cords and cultured as previously described [2]. At confluence, medium was replaced with a 50/50 cocktail of HUVEC growth medium and test medium. HUVEC were stimulated for a period of 4 hours for E/P-selectin or 16 hours for ICAM-1 and VCAM-1 expression analysis. HUVEC were then detached using trypsin/EDTA and analysed by flow-cytometry as previously described [3]. Endothelial activation markers were expressed as the relative fluorescent intensity (RFI), where a value of 1.00 is equivalent to no antigen expression) calculated by dividing the mean fluorescent intensity of the test antibody on any given day by the staining intensity of the isotype-matched control antibody on the same day. Results were expressed as the mean ± SEM RFI from 2-3 separate experiments.

Hydrodynamic shear flow adhesion assay

HUVEC were grown to confluence in 9cm^2 slide flaskettes (Nalge Nunc International) and then mounted in a parallel-plate flow chamber (channel height 0.15cm). Human peripheral blood mononuclear cells (PBMCs) were prepared from fresh citrated blood by centrifugation over a Ficoll-Hypaque (Pharmacia Biotech) gradient as previously described [4]. PBMCs were labelled with calcein-AM (Molecular Probes, Eugene, OR) and perfused at 37°C over mounted HUVEC monolayers at a wall shear stress of 1.5 dynes/cm^2. Experiments were analyzed to determine the number of rolling and adherent cells per field as previously described [5]. Results are expressed as the mean ± SEM of rolling or adherent cells from four different experiments.

Western blot analysis

Western blot analysis was performed by SDS-PAGE and semidry transfer onto a PDVF membrane as previously described [2]. The membrane was probed by incubating overnight at 4ºC with the primary antibody followed by detection with the secondary HRP-conjugated antibody and ECL chemiluminescence detection kit (Amersham Pharmacia Biotech, UK). For quantification of western blot bands densitometry was performed using an Alpha Innotech ChemiImager 5500 (Alpha Innotech, San Leandro, CA). Integrated density values (IDV) for the test and control bands were obtained and demonstrated as their ratio.

Adenovirus amplification, purification and titration

Recombinant, replication-deficient adenoviral vectors encoding green fluorescent protein (GFP) and a PKCα kinase negative mutant ($_{368}K \rightarrow R$) [6] were generously provided by Dr.Ewa Paleolog (Kennedy Institute of Rheumatology, Imperial College London, UK) and Dr Motoi Ohba (Institute of Molecular Oncology, Showa University, Tokyo, Japan) respectively. Both viruses are (E1/E3) early transcribed regions deleted and belong to the Adv5 serotype. Viruses were propagated in the E1 gene complementing 293 human embryonic kidney cell line (American Type Culture Collection, Rockville, MD) and were purified chromatographically using the BD Adeno-X™ virus purification kit (BD Biosciences, Oxford, UK) according to manufacturers instructions. Titres of viral stocks were determined using an anti-viral hexon protein ELISA viral titration method based on 293 HEK infected cells using the BD Adeno-X™ Rapid Titre kit (BD Biosciences, Oxford, UK) as per manufacturers instructions.

Preparation of monocyte derived macrophages for adenoviral infection

Adenovirus infection was performed using a modification of a method previously

described [7]. In brief human monocytes were cultured for 4 days on 60cm^2 tissue culture Petri dishes (Nunc-Nalge, Hereford, UK) in standard macrophage growth medium, containing 10% autologus serum with the addition of 100ng/ml of M-CSF (Peprotech EC, London, UK). Adherent cells were then detached by rinsing once with HBSS (without cations) and incubating with 5mls of Cell Dissociation Medium (Sigma) for 1 hour at 37°C. Detached cells were washed twice and reseeded at 0.5x10^6 cells/well on a 24 well plate (Nunc-Nalge, Hereford, UK) in macrophage growth medium (minus M-CSF) and allowed to re-adhere overnight at 37°C, 5% CO_2. Macrophages were then rinsed and medium replace with serum-free macrophage growth medium. Macrophages were innoculated with adenovirus and infection was allowed to take place for 2 hours at 37°C, 5% CO_2 before replacing infected with fresh growth medium. Cells were cultured for a further two days to allow for significant over-expression of protein, prior to stimulation with BCP crystals. Using this method a maximal macrophage infection efficiency of 80% was achieved with a multiplicity of infection (MOI) of 400:1, as determined by FACS (FL1 channel-460nm) analysis of GFP-adenovirus infected macrophages.

ONLINE FIGURE LEGENDS

Online Figure I. X-Ray elemental microanalysis Further evidence that the structures contained in vacuoles detected by transmission electron microscopy were BCP crystals was obtained using X-ray elemental microanalysis. Cells treated with media control demonstrated an abundance of intracellular phosphate (online Figure IA, peak 1), which is the predominant element found in all mammalian cells. Cells treated with BCP particles (300μg/cm^2) demonstrated a phosphate peak (online Figure

IB, peak 1) and an additional calcium peak (online Figure IB, peak 2). This calcium peak is likely to be due to BCP crystals. See above for Methods.

Online Figure II. BCP crystals cultured with macrophages but separated by a semi-permeable membrane did not induce release of TNFα. Macrophages were cultured for 20 hours in contact with BCP crystals or separated by a semipermeable membrane in a tissue culture insert (0.02μm Anopore membrane, Nalge Nunc International, Roskilde, Denmark). The results showed that macrophages needed to contact BCP crystals for TNFα release to occur. Statistical analysis was using a One-way ANOVA with a Dunnetts post test.

Online Figure III. Supernatants from BCP crystal-treated macrophages fail to induce TNFα mRNA in fresh macrophages. Macrophages were stimulated for 6 hours with medium control, BCP crystals (300μg/cm^2) or with centrifuged conditioned media (14,000rpm for 10 minutes at 4ºC) from macrophages treated for 20 hours with medium or BCP (300μg/cm^2) crystals. Steady state mRNA levels were then measured using quantitative RT-PCR gene expression analysis. Data are expressed as mRNA levels relative to unstimulated control cells. Statistical analysis using a One-way ANOVA with a Dunnetts post test.

Online Figure IV. Supernatants from BCP crystal-treated macrophages activate endothelial cells. HUVEC were incubated with conditioned media from human macrophages previously treated for 20hrs with media (vehicle control) or BCP. (**A**) flow-cytometric expression of adhesion molecules (E-selectin at 4 hours n=3, VCAM-

1 and ICAM-1 at 16 hours, n=2) is shown as the relative fluorescent intensity (RFI). The RFI was calculated by dividing the staining intensity (mean fluorescent intensity [MFI]) of the test antibody on any given day by the staining intensity of the class-matched control antibody on the same day. A value of 1.00 is equivalent to no antigen expression. All results were expressed as the mean ± SEM RFI from 2-3 separate experiments. (**B**) dynamic rolling and adhesive interactions of mononuclear cells recorded in a hydrodynamic shear flow assay. Confluent HUVEC mono-layers were pre-treated for 16hrs with the conditioned media collected from macrophages (vehicle control or BCP stimulated) prior to perfusion of mononuclear cells (n=4).

Reference List

(1) Livak KJ, Schmittgen TD. Analysis of relative gene expression data using real-time quantitative PCR and the 2(-Delta Delta C(T)) Method. *Methods* 2001;25:402-8.

(2) Mason JC, Yarwood H, Tarnok A, Sugars K, Harrison AA, Robinson PJ, Haskard DO. Human Thy-1 is cytokine-inducible on vascular endothelial cells and is a signaling molecule regulated by protein kinase C. *J Immunol* 1996;157:874-83.

(3) Landis RC, Yagnik DR, Florey O, Philippidis P, Emons V, Mason JC, Haskard DO. Safe disposal of inflammatory monosodium urate monohydrate crystals by differentiated macrophages. *Arthritis Rheum* 2002;46:3026-33.

(4) Landis RC, Friedman ML, Fisher RI, Ellis TM. Induction of human monocyte IL-1 mRNA and secretion during anti-CD3 mitogenesis requires two distinct T cell-derived signals. *J Immunol* 1991;146:128-35.

(5) Rao RM, Clarke JL, Ortlepp S, Robinson MK, Landis RC, Haskard D.O. The S128R polymorphism of E-selectin mediates neuraminidase-resistant tethering of myeloid cells under shear flow. *Eur J Immunol* 2002;32:251-60.

(6) Ohba M, Ishino K, Kashiwagi M, Kawabe S, Chida K, Huh NH, Kuroki T. Induction of differentiation in normal human keratinocytes by adenovirus-mediated introduction of the eta and delta isoforms of protein kinase C. *Mol Cell Biol* 1998;18:5199-207.

(7) Foxwell B, Browne K, Bondeson J, Clarke C, de MR, Brennan F, Feldmann M. Efficient adenoviral infection with IkappaB alpha reveals that macrophage tumor necrosis factor alpha production in rheumatoid arthritis is NF-kappaB dependent. *Proc Natl Acad Sci U S A* 1998;95:8211-5.

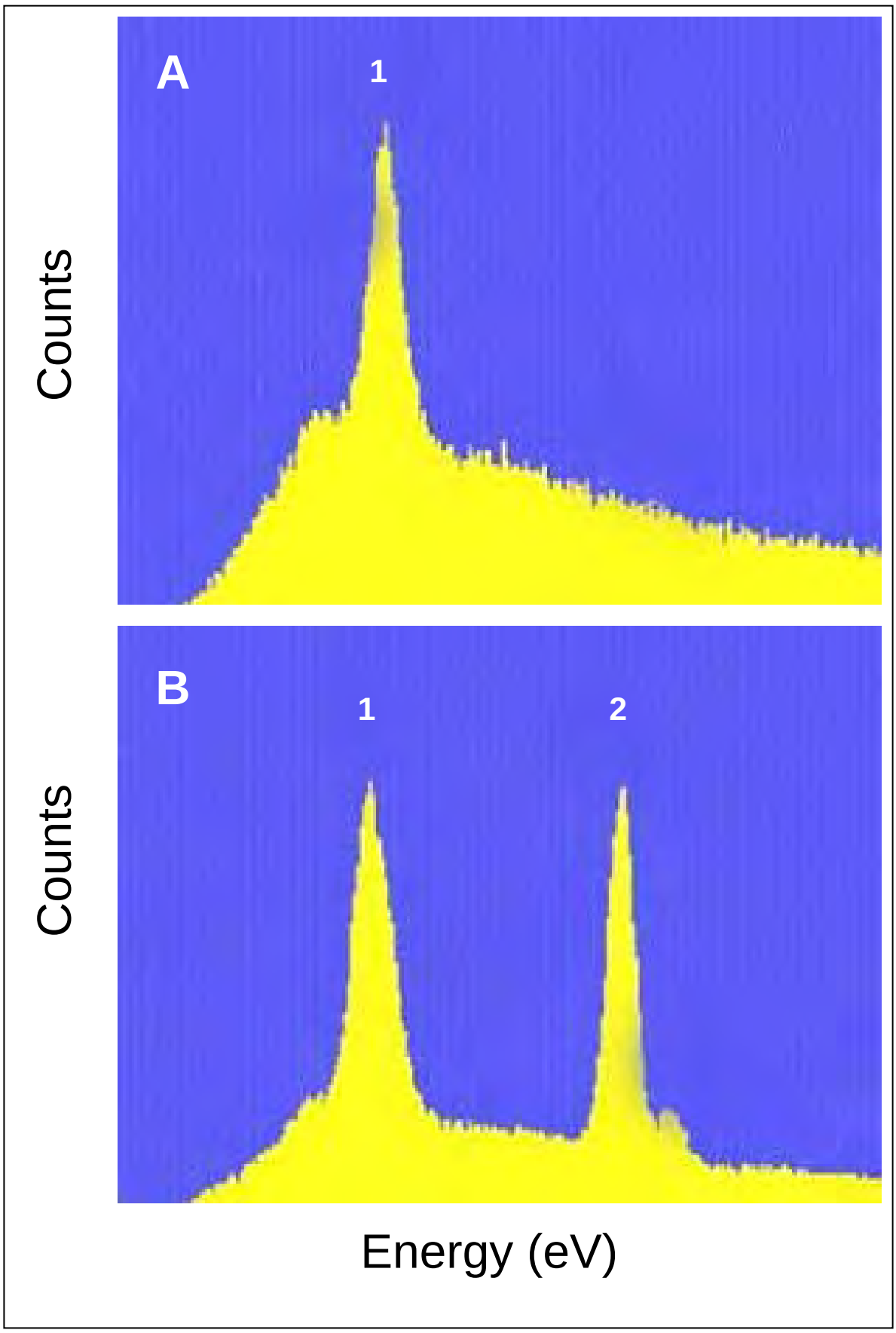

Online Figure I

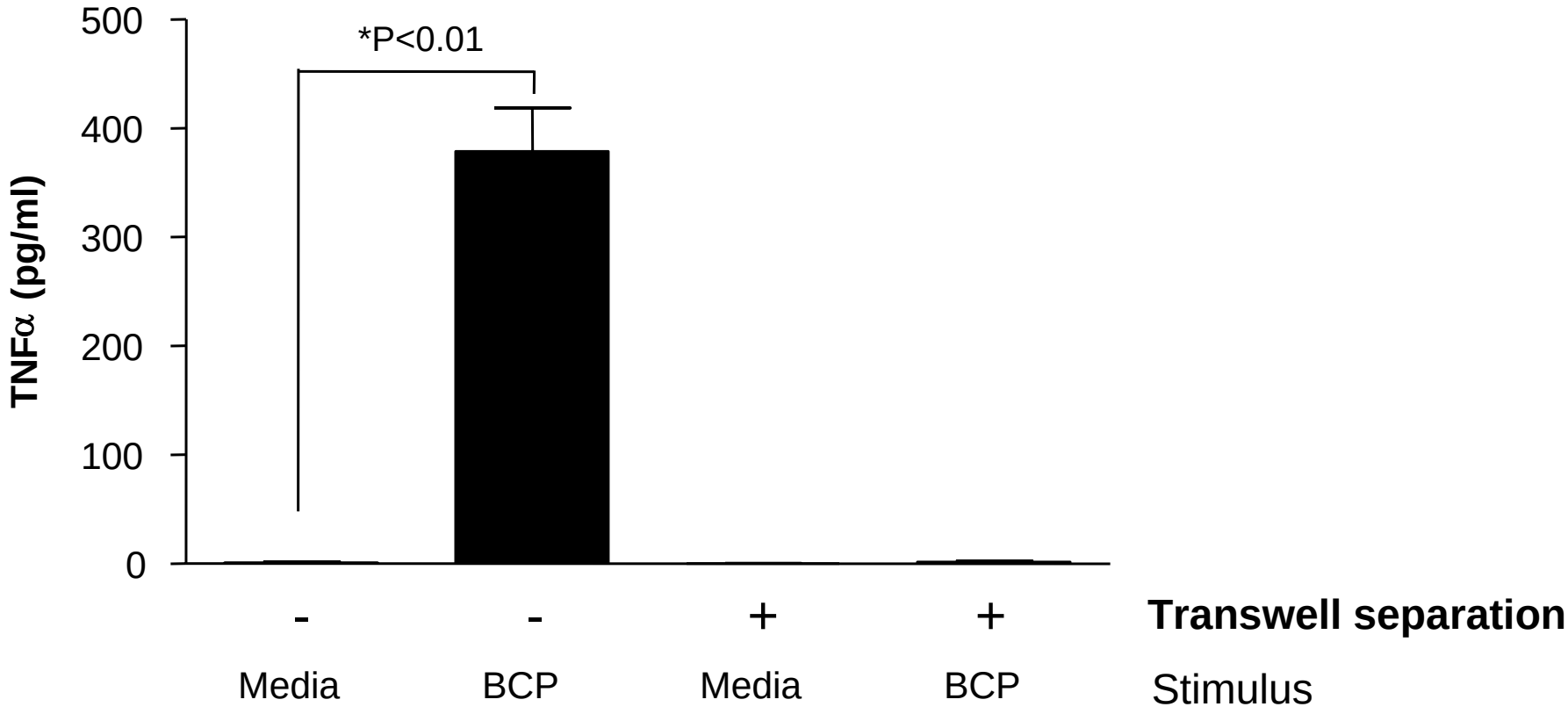

Online Figure II

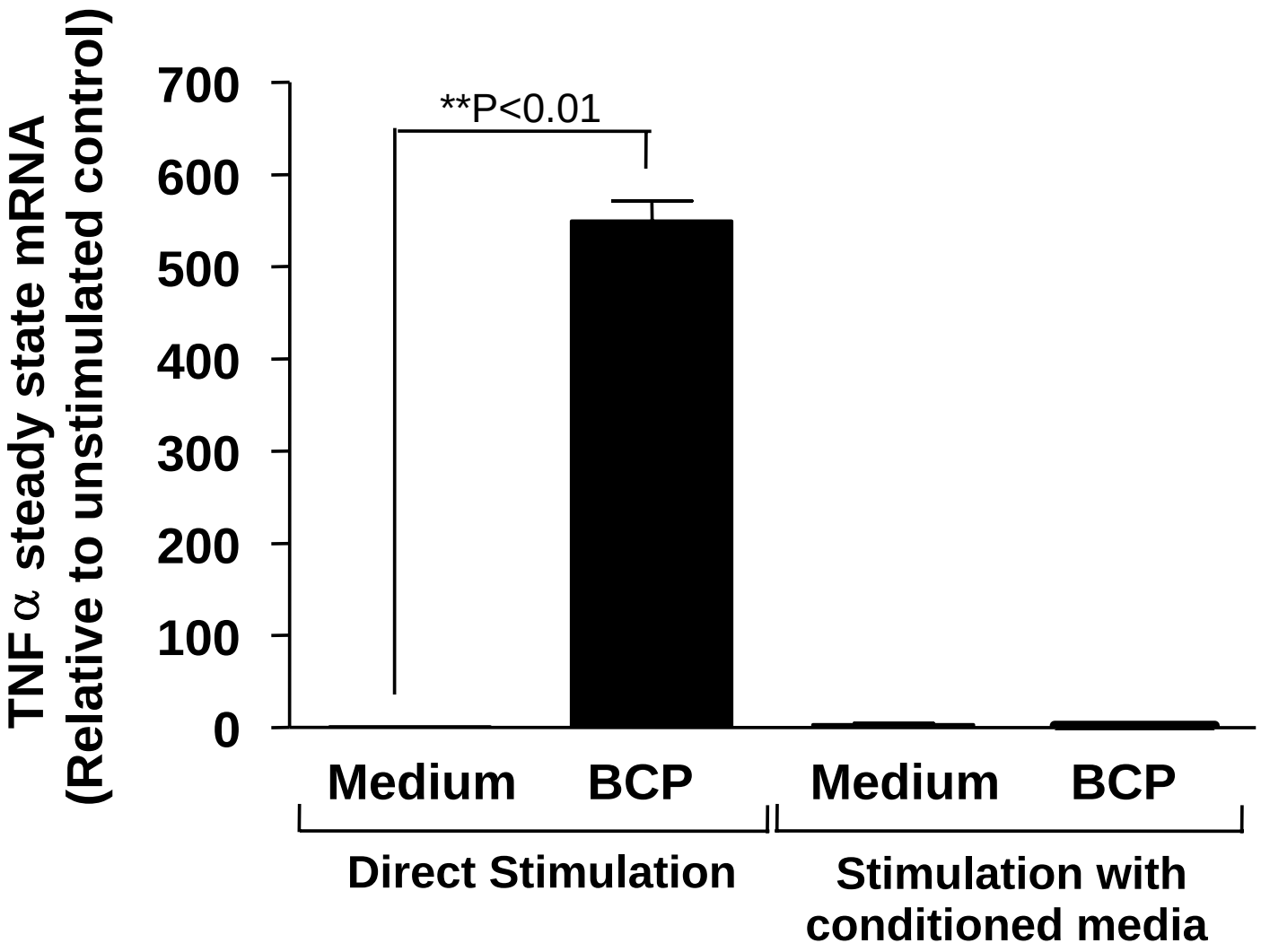

Online Figure III

A

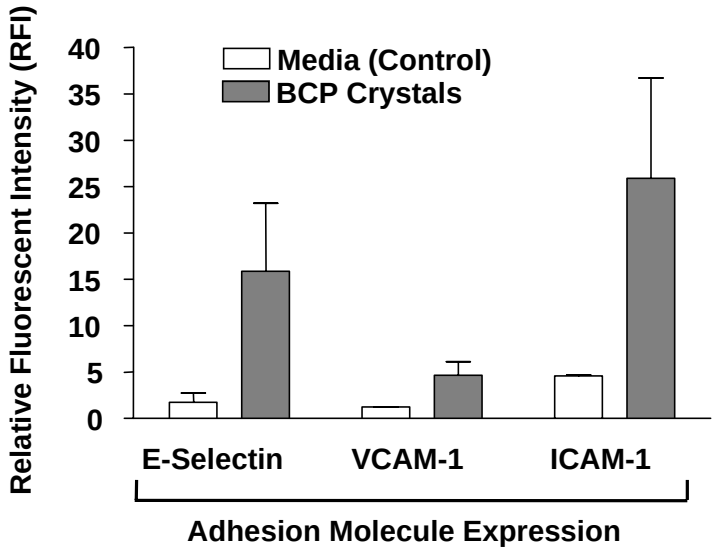

B

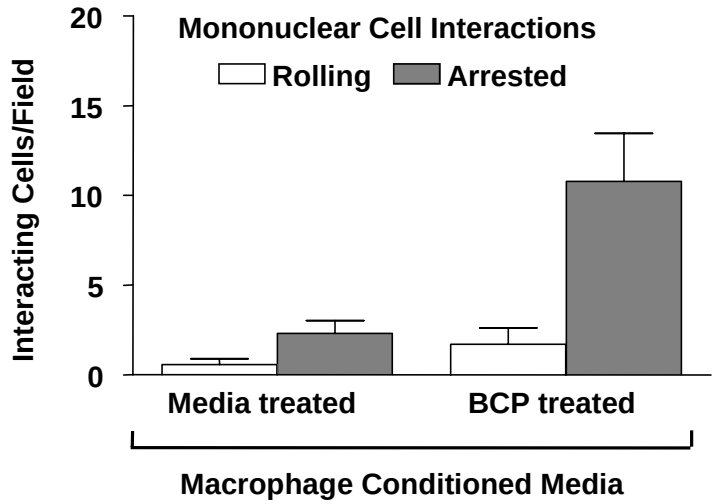

Online Figure IV

Proinflammatory Activation of Macrophages by Basic Calcium Phosphate Crystals via Protein Kinase C and MAP Kinase Pathways: A Vicious Cycle of Inflammation and Arterial Calcification?

Imad Nadra, Justin C. Mason, Pandelis Philippidis, Oliver Florey, Cheryl D.W. Smythe, Geraldine M. McCarthy, Robert C. Landis and Dorian O. Haskard

Circ Res. 2005;96:1248-1256; originally published online May 19, 2005;
doi: 10.1161/01.RES.0000171451.88616.c2
Circulation Research is published by the American Heart Association, 7272 Greenville Avenue, Dallas, TX 75231

Print ISSN: 0009-7330. Online ISSN: 1524-4571